Iranian Journal of Oil & Gas Science and Technology, Vol. 7 (2018), No. 2, pp. 79-90
http://ijogst.put.ac.ir

Catalytic Oxidation of Carbon Monoxide by Cobalt Oxide Catalysts Supported on Oxidized-MWCNT

Mahnaz Pourkhalil[1*] and Saeideh Tasharrofi[2]

[1] Assistant Professor, Nanotechnology Research Center, Research Institute of the Petroleum Industry, Tehran, Iran
[2] M.S. Student, Environmental and Biotechnology Department, Research Institute of the Petroleum Industry, Tehran, Iran

Received: November 15, 2017; *revised*: November 28, 2017; *accepted*: December 11, 2017

Abstract

Cobalt oxide catalysts supported on oxidized multi-walled carbon nanotubes (MWCNT) for the low-temperature catalytic oxidation of carbon monoxide were prepared by an impregnation-ultrasound method. These catalysts were characterized by N_2 adsorption/desorption, TEM, XRD, Raman, and H_2-TPR methods. The XRD and Raman results indicated that the phase of the synthesized cobalt oxide was in the Co_3O_4 form. The effects of cobalt oxide loading and reaction temperature were studied on the catalytic oxidation conversion of carbon monoxide. The TEM image of the best catalyst (14 wt.% metal oxide loading) revealed a good dispersion of Co_3O_4 over the surface of the support with an average particle size of 11-16 nm. Under the reaction conditions of T= 200-250 °C, P= 1 bar, CO = 600 ppm, O_2 = 5 vol.%, GHSV = 30,000 $hr.^{-1,}$ and Co_3O_4= 14 wt.%, CO conversion was 91%.

Keywords: Co_3O_4, Oxidized Multi-walled Carbon Nanotubes, Carbon Monoxide, Oxidation

1. Introduction

CO from the exhaust gases of automobiles and combustion engines remains one of the most serious pollutants (Chai et al., 2017; Lv et al., 2016). A well-proven method for CO abatement is the catalytic oxidation of CO to carbon dioxide due to its economic advantages and simplicity (Lee et al., 2016; Dong et al., 2017). Although noble metal catalysts with/without different supports, including Au-CeO_2 (Bansmann et al., 2017), gold nanoparticles (Qiao et al., 2016), Pd/TiO_2 (Bratan et al., 2017), Pd/SnO_2 (Jin et al., 2012) exhibit a high activity in this reaction, the high cost and easily sintering limit their extensive applications (Chai et al., 2017). Among the non-precious metal catalysts, transition metal oxide catalysts such as Co_3O_4 (Wang et al., 2017), CuO (Wang et al., 2017), and Fe_2O_3 (Cui et al., 2017) have attracted much attention in the catalytic oxidation reaction of CO due to their high activity and thermal stability (Bao et al., 2011). Some research findings have shown that the catalytic activity and redox property of Co_3O_4 are strongly influenced by the formation of oxygen vacancies (Zhang et al., 2017; Chen et al. 2017), controlling the crystalline size (Kant Sharma et al., 2017) and its oxidation state (Chen et al., 2016). Therefore, the performance of cobalt oxide, which is one of the most promising catalysts for the complete oxidation of CO, appears to be critically

[*] Corresponding Author:
Email: pourkhalilm@ripi.ir

dependent on the preparation method (Yuan et al., 2017; Liu et al., 2017) and the nature of the support (Wang, 2016).

Carbon nanotubes have proved attractive and competitive as a catalyst support in heterogeneous catalytic reactions due to their distinctive morphology, high thermal resistance, and conductivity (Payan et al., 2018; Fattahi et al., 2015; Liu et al., 2018; Zhou et al., 2017). CNTs, with the unique one-dimensional tubular and mesoporous structure, simplify the transmission of reactants and products in chemical reactions (Huang et al., 2007; Santillan-Jimenez et al., 2011). CNTs have a hydrophobic surface with low solubility and dispersivity in polar solvents (Mazov et al., 2012). The introduction of oxygenated groups such as (OH and COOH) to CNT surface has been reported to increase the wetting characteristics of CNTs and to increase the dispersion of metal particles on their surface (Kundu et al., 2008). These oxygenated groups can bond metal oxides onto the CNT surface (Chuang et al., 2011). Gao and coworkers (Gao et al., 2015) have reported that CuO-CeO_2 catalyst supported on OMWNTs, with the nominal ratio of Cu to Ce equal to 5/5 and a total metal oxide loading of 20 wt.%, had a high activity and selectivity for PROX of CO in comparison with CuO-CeO_2 catalysts supported on other materials, including activated carbon, γ-Al_2O_3, and SiO_2 in an H_2-rich stream. In this work, cobalt oxide catalysts supported on OMWNTs were prepared by an ultrasound-assisted impregnation method, and their performance was tested for the catalytic oxidation of CO at low temperatures. The effects of CoOx loading and reaction temperature on conversion and selectivity were also studied. Phase transformation, redox, and structural properties were characterized by N_2 adsorption/desorption, XRD, Raman, TEM, and H_2-TPR techniques.

2. Experimental

2.1. Catalyst preparation and characterization

a. Oxidation of the support

The employed MWNTs (95% purity, 10–30 nm in OD) were prepared by a chemical vapor deposition (CVD) method over a Co–Mo/MgO catalyst at Research Institute of the Petroleum Industry (RIPI), Iran (Rashidi et al., 2007). Following the purification of the raw MWNTs, they were oxidized in a 1:3 (v/v) solution of HNO_3 (65%) and H_2SO_4 (98%) in an ultrasonic bath (Fisher Scientific, 130 W and 40 kHz) maintained at 60 °C for 2 hrs. The solution was then filtered, and washed using de-ionized water to remove excess acid; it was then dried in the oven at 110 °C in air for 24 hrs (Xing et al., 2005).

b. Catalyst preparation

Supported cobalt oxide catalysts at different loadings (2–18 wt.%) were prepared by the impregnation technique aided by ultrasonic treatment. The OMWNTs were impregnated using certain amounts of an aqueous solution of $Co(NO_3)_2\ 6H_2O$ as the precursor for cobalt oxide. The solutions were subjected to an ultrasonic treatment for 1 hr. Afterwards, the samples were first dried in a rotary evaporator at 78 °C and then in an oven at 100 °C for 24 hrs. Loading of cobalt oxide on the OMWNTs was controlled by adjusting the ratio between the OMWNTs and cobalt nitrate. The catalysts were calcined in a tubular furnace at 400 °C for 3 hrs under a blanket of argon as a carrier gas to obtain CoOx/OMWNTs catalysts at different loadings.

c. Catalyst characterization

The specific surface areas of the support and catalysts were measured by nitrogen adsorption at -196 °C with the BET method on a Belsorp II (BEL Co., Japan) instrument. The samples were degassed at 250 °C

for 3 hrs under vacuum. Total pore volume and mean pore diameter of the samples were calculated from adsorption and desorption isotherms at a relative pressure ($P/P°$ of 0.98). The crystalline phase of the support and cobalt oxides over the OMWNTs was characterized by XRD. The measurements were obtained using an X'Pert MPD-PHILIPS X-ray diffractometer with Cu Ka (k = 1.5056 Å) radiation. The voltage and current of the anode were 40 kV and 30 mA respectively. The scanning range of 2θ was from 5 to 70 ° with a step size of 0.04 °/s. The diffraction patterns were manually analyzed with the Joint Committee of Powder Diffraction Standard (JCPDS) card. Raman spectra were employed at ambient temperature on an Almega Thermo Nicolet Dispersive Raman Spectrometer with an argon-ion laser at an excitation wavelength of 514 nm. The TEM observations were made with a Zeiss EM900 microscope operated at 120 keV to observe the dispersion of active sites on the support surface. The samples were prepared by the ultrasonic dispersion of the catalysts in ethanol, and the suspensions were then dropped onto a carbon-coated copper grid. The temperature programmed reduction (TPR) experiments were performed on a Micromeritics-2900 system equipped with a thermal conductivity detector (TCD). 50 mg of the catalyst was reduced in a flow of 5% H_2 under the blanket of argon at a flow rate of 40 cc min^{-1} and at a linear heating rate of 10 °C min^{-1} from 25 to 800 °C.

2.2. Catalytic activity tests

The CO oxidation experiments were carried out in a fixed bed quartz reactor at atmospheric pressure between 100 and 250 °C. The gas composition was 600 ppm CO and 5 vol.% O_2 balanced with He as the carrier gas. Before adding the reactant gas into the reactor, the gases were mixed in a glass chamber. In all the tests, the total flow rate was fixed at 500 $cc.min^{-1}$, which corresponds to a GHSV of 30,000 $hr.^{-1}$. CO and O_2 concentrations in the inlet and outlet gases were measured using an on-line flue gas analyzer (Testo model 340, Germany) equipped with CO and O_2 sensors (Figure 1). The reaction temperature was controlled by a K-type thermocouple inserted directly into the catalyst bed. The catalytic activity was calculated by the following equation:

$$\mathrm{Xco\%} = \frac{[\mathrm{CO}]\mathrm{in} - [\mathrm{CO}]\mathrm{out}}{[\mathrm{CO}]\mathrm{in}} \times 100\% \quad (1)$$

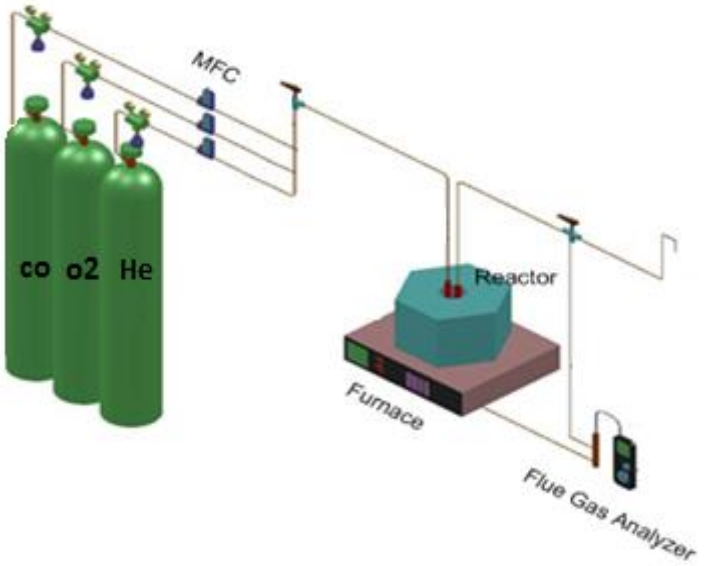

Figure 1
A schematic of the activity test system.

3. Results and discussion

3.1. Effect of reaction temperature

The activity of the support and the 14 wt.% CoOx/OMWNTs in the CO oxidation at reaction temperatures between 100 and 250 °C is detailed in Figure 2. In this temperature range, CO conversion on the OMWNTs was very low (5–6%, Figure 2a), which could be attributed to the CO adsorption by carbon nanotubes (Azizi et al., 2011). As the temperature increased, the CO conversion increased from 55% at 100 °C to 83% at 150 °C; it finally reached a maximum conversion of 91% at temperatures more than 200 °C (Figure 2b); thus, the optimum low reaction temperature over CoOx/OMWNTs for CO oxidation was 200 °C.

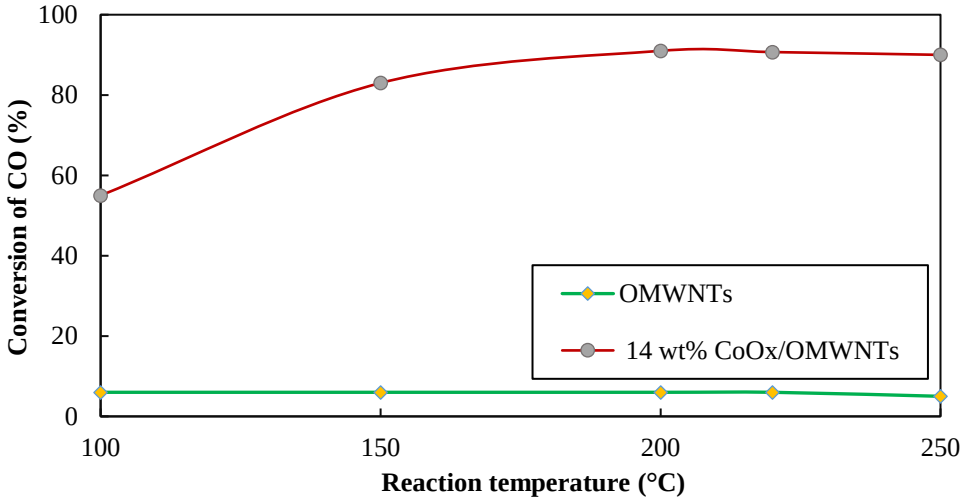

Figure 2
Effect of reaction temperature on CO conversion of a) OMWNTs and b) 14 wt.% CoOx/OMWNTs.

3.2 Effect of CoOx loading

The effect of different cobalt oxide loadings (2–18 wt.%) on CO conversion is displayed in Figure 3. Over all the reaction temperatures, changing the CoOx loadings from 2 to 14 wt.% resulted in an increased conversion due to an increased number of active sites. By increasing CoOx loading over the support to 18 wt.%, the agglomeration of the active sites occurred, and the catalyst activity declined.

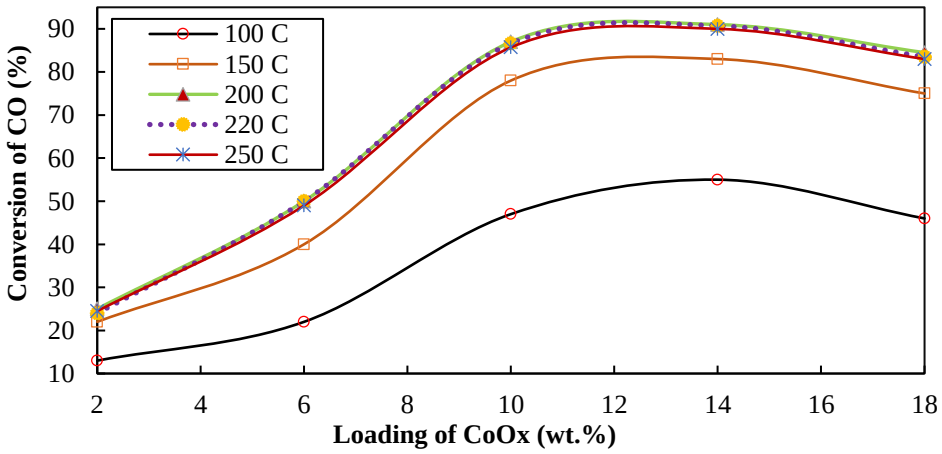

Figure 3
Effect of CoOx loading at different reaction temperatures on CO conversion.

The surface area, total pore volume, and mean pore diameter of the OMWNTs and 10 wt.%, 14 wt.%, and 18 wt.% CoOx/OMWNTs are tabulated in Table 1. After impregnation, the surface area of the catalysts increased, but the pore volume and pore diameter dropped by the formation of cobalt oxide nanoparticles on the support. On increasing the cobalt loading from 10 to 14 wt.%, the changes in total pore volume and mean pore diameter were negligible, whereas the catalyst had the maximum surface area (208 $m^2gr.^{-1}$) (see Table 1).

Table 1
Surface area, total pore volume, and mean pore diameter of OMWNTs and CoOx/OMWNTs.

Samples	S_{BET} ($m^2gr.^{-1}$)	Total pore volume ($cm^3gr.^{-1}$)	Mean pore diameter (nm)
OMWNTs	185.8	0.86	18.56
10 wt.% cobalt oxide	199.2	0.69	13.38
14wt.% cobalt oxide	208	0.65	13.39
18 wt.% cobalt oxide	191.3	0.53	10.95

A TEM image of cobalt oxide nanoparticles (14 wt.%) over OMWNTs in Figure 4a shows a good dispersion of the active phase on the surface of the support with an average particle size of 11-16 nm. However, the surface area, pore volume, and pore diameter of the 18 wt.% CoOx catalyst were all decreased due to the agglomeration of CoOx. A TEM image of the 18 wt.% CoOx catalyst is illustrated in Figure 4b. Figure 5 depicts the XRD patterns of the pure cobalt oxide (prepared by the ultrasonic-assisted impregnation method), OMWNTs, and CoOx/OMWNTs (10 wt.%, 14 wt.%, and 18 wt.%).

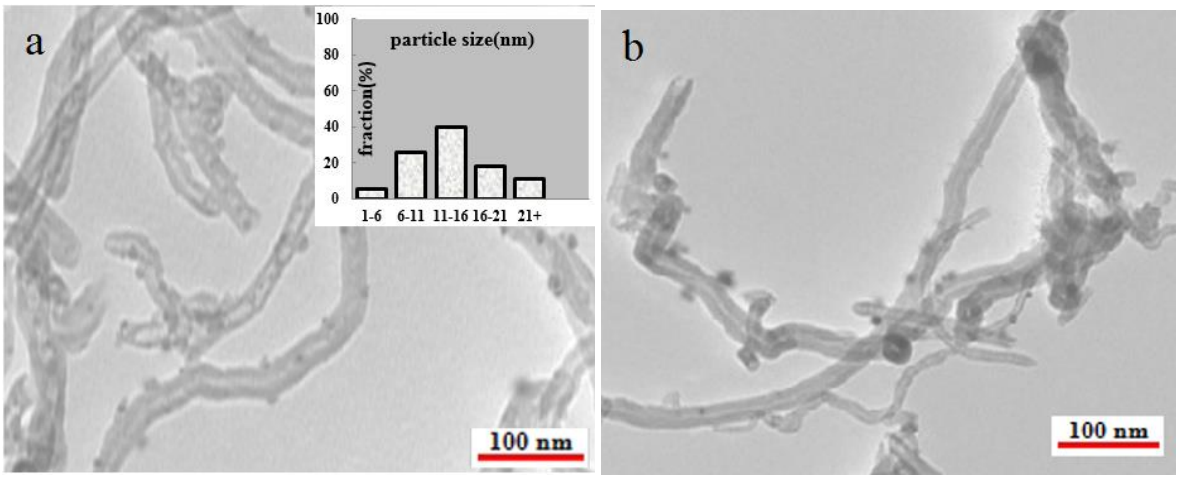

Figure 4
TEM image of a) 14 wt.% CoOx/OMWNTs and b) 18 wt.% CoOx/OMWNTs.

Over the pure cobalt oxide (Figure 5a), diffraction peaks observed at 17.0, 30.3, 36.8, 39.0, 46.2, 59.4, and 64.2 ° can be indexed as (1 1 1), (2 2 0), (3 1 1), (2 2 2), (4 0 0), (5 1 1), and (4 4 0) lattice planes of spinel Co_3O_4 (JCPDS no ≠ 76-1802) respectively. No diffraction peaks corresponding to CoO or Co phases are observed. Figure 5b displays the peaks at 2θ of 25.7, 41.9, 43.16, and 50.9° for the (002), (100), (101), and (004) diffractions of graphite (JCPDS # 08-0415), indicating that the structure of the MWNTs support was not destroyed through the ultrasonic treatment (Belin and Epron, 2005).

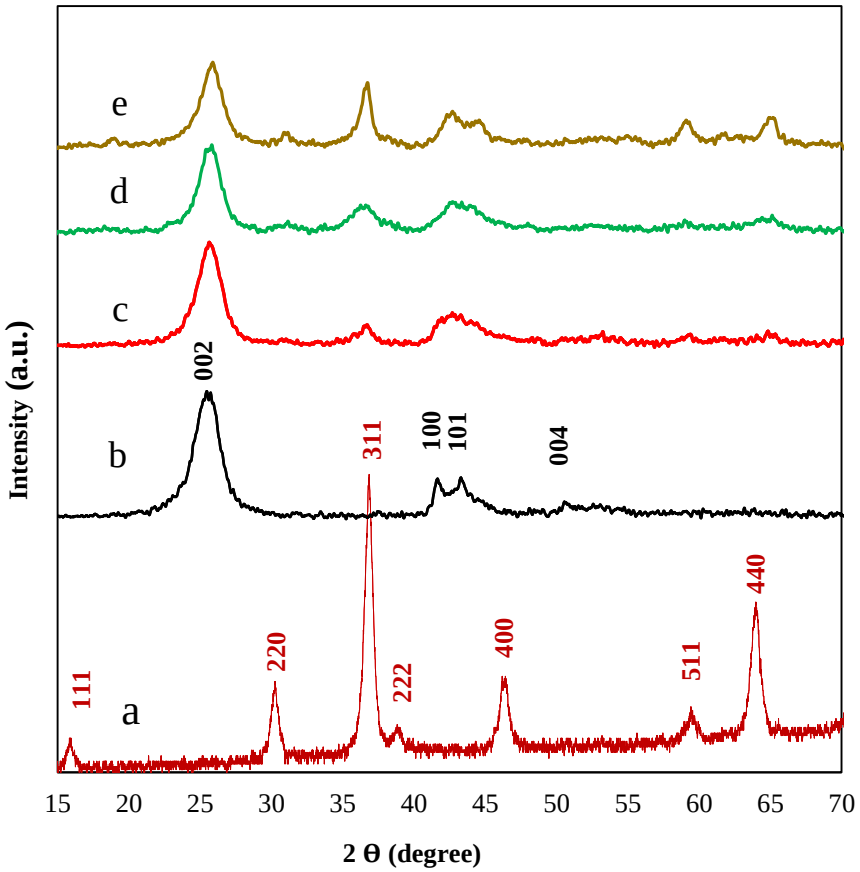

Figure 5
XRD patterns of a) cobalt oxide, b) OMWNTs, and c) CoOx/OMWNTs catalysts 10 wt.% loadings, d) CoOx/OMWNTs catalysts 14 wt.% loadings, and e) CoOx/OMWNTs catalysts 18 wt.% loadings.

Over CoOx/ OMWNTs, the intensity of Co_3O_4 peaks increased slightly at higher cobalt loadings. The Raman spectra of MWNTs, OMWNTs, and 14 wt.% cobalt oxide are drawn in Figure. 6. It can be seen that MWNTs have two main peaks at about 1345 and 1567 cm^{-1} (Figure 6a). The peak around 1345 cm^{-1} (D-band) is associated with the vibrations of carbon atoms in the disordered graphite structure, i.e., the defects. The G-band is due to the first order scattering of the E_{2g} mode of graphite. Therefore, the ratio of D-band intensity to G-band (I_D/I_G) is related to the defect density in carbon nanotubes and provides direct information on the oxidation degree of carbon nanotubes (Zou et al., 2008; Chaunchaiyakul et al., 2016). As shown in Figure 6, the I_D/I_G ratio of the OMWNTs is higher than that of MWNTs, confirming the formation of defect sites by the addition of the oxygen groups. The Raman scattering reflections in Figure 6c at 482 cm^{-1} is ascribed to the E_g mode of Co_3O_4, and the reflections at about 520 and 625 cm^{-1} are attributed to F_{2g}; the reflection at 695 cm^{-1} stands for the A_{1g} mode of Co_3O_4 (Pu et al., 2017). These results confirm the existence of the crystalline structure of cobalt oxide in the Co_3O_4 form, which is in agreement with the XRD results. Decreasing the I_D/I_G ratio of the OMWNTs from 1.21 to 1.17 in the 14 wt.% catalyst can be attributed to the anchoring of cobalt oxide nanoparticles onto the defect sites of OMWNTs.

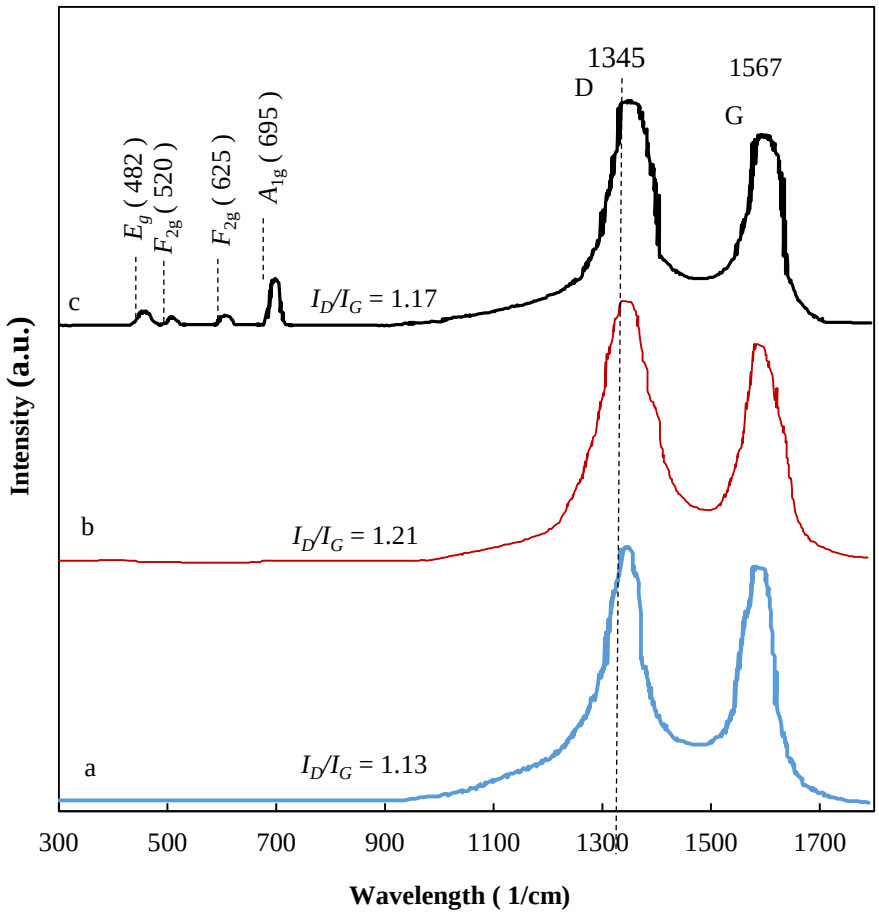

Figure 6
Raman spectra of a) MWNTs, b) OMWNTs, and c) 14 wt.% cobalt oxide/OMWNTs.

Figure 7 displays the H_2-TPR analysis of the pure cobalt oxide, OMWNTs, and CoOx/OMWNTs (10 wt.%, 14 wt.%, and 18 wt.%) to investigate their reduction behavior. The TPR profile of the cobalt oxide with two typical reduction peaks is plotted in Figure 7a, which indicates a two-step reduction process of Co_3O_4 to CoO at about 250–350 °C and CoO to metallic cobalt in the region of 350–560 °C according to Equations 2 and 3 (Tang, Wang and Chien, 2008):

$$Co_3O_4 + H_2 \longrightarrow 3CoO + H_2O \quad (2)$$

$$CoO + H_2 \longrightarrow Co + H_2O \quad (3)$$

Xia et al. (Xia et al., 2010) found out that the reduction profile of Co_3O_4 includes a low-temperature peak in the range of 200–350 °C and a high-temperature peak at approximately 500 °C. With respect to the H_2-TPR profile of the catalysts (10 wt.%, 14 wt.%, and 18 wt.%) in Figures 7c, 7d, and 7e, the existence of these two main peaks proves the presence of cobalt oxide in the form of Co_3O_4, which is in agreement with the results reported by XRD (Figure 5) and Raman (Figure 6) studies. Comparing the profile of the support (Figure 7b) with that of the catalysts (Figures 7c, 7d, and 7e), the increase in the temperature range of the second peak to 750 °C can be attributed to the carbon methanation of the support in the presence of hydrogen at high temperatures (> 500 °C) (Xiong et al., 2013).

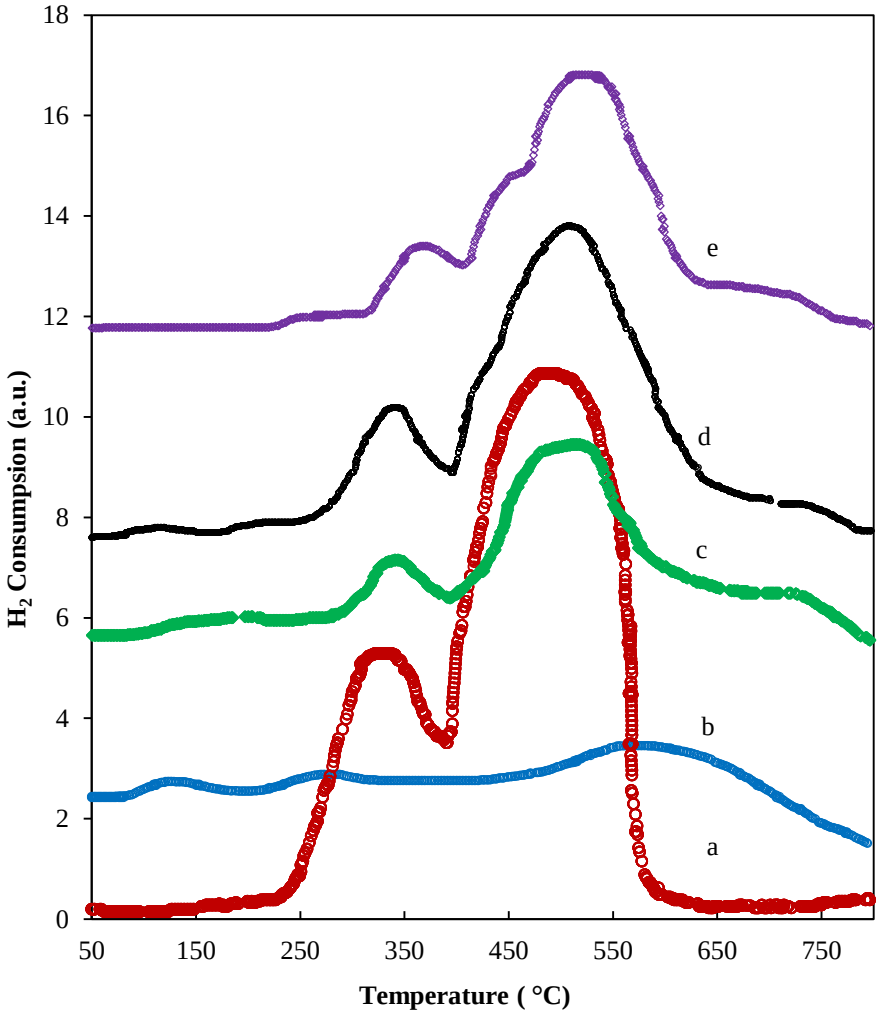

Figure 7
H2-TPR profile of a) cobalt oxide, b) OMWNTs, c) 10 wt.% cobalt oxide catalyst, d)14 wt.% cobalt oxide catalyst, and e) 18 wt.% cobalt oxide catalyst.

4. Conclusions

A series of CoOx over oxidized multi-walled carbon nanotube catalysts have been prepared by an impregnation-ultrasound method at different loadings (2-18 wt.%). The activity of the prepared catalysts was examined for the catalytic oxidation of carbon monoxide. The effects of CoOx loading and reaction temperature on CO conversion were also discussed. Increasing CoOx loading from 2 to 14 wt.% increased conversion, while higher loadings to 18 wt.% led to the agglomeration of cobalt oxide particles and increased catalyst crystallinity. The XRD and Raman profiles of the catalysts confirmed that the cobalt oxide was in the form of Co_3O_4, which is very active in redox reactions. The catalyst having 14 wt.% metal loading had the highest surface area and a good dispersion of Co_3O_4 in the range of 11-16 nm; in addition, it exhibited the maximum catalytic performance toward the oxidation of CO into CO_2 at about 91% at temperatures more than 200 °C. Under the objective to evaluate the capability of the prepared catalyst for CO removal from exhaust gases of stationary sources, in reality, simultaneously investigating the catalyst efficiency in the presence of water vapor, SO_2, and NO_X emissions are suggested. Finally, in order to increase the thermal stability of the catalyst at high temperatures, our studies will focus on usage of carbon-metal oxide hybrid supports in the future.

Nomenclature

BET	: Brunauer–Emmett–Teller
CNTs	: Carbon nanotubes
CO	: Carbon monoxide
COOH	: Carboxyl
CoOx	: Cobalt oxide
GHSV	: Gas hourly space velocity
H_2-TPR	: H_2-temperature-programmed reduction
JCPDS	: Joint Committee on Powder Diffraction Standards
OD	: Outside diameter
OH	: Hydroxyl
OMWNTs	: Oxidized multi-walled carbon nanotubes
PPROX	: Preferential oxidation
Redox	: Reduction-oxidation
TEM	: Transmission electron microscopy
X_{CO}	: Conversion of CO
XRD	: X-ray powder diffraction

References

Azizi, K., Hashemianzadeh S. M., and Bahramifar, S., Density Functional Theory Study of Carbon Monoxide Adsorption on the Inside and Outside of the Armchair Single-walled Carbon Nanotubes, Current Applied Physics Vol. 11, No. 3, p. 776-782, 2011.

Bansmann, J., Kucerova, G., Abdel-Mageed, A. M., Abd El-Moemen A., and Behm, R. J., Influence of Re-activation and Ongoing CO Oxidation Reaction on the Chemical and Electronic Properties of Au on an Au/CeO_2 Catalyst: A XANES Study at the Au LIII Edge, Journal of Electron Spectroscopy and Related Phenomena, Vol. 220 (Supplement C), p.86-90, 2017.

Bao, H., Zhang, W., Hua, Q., Jiang, Z., Yang, J., and Huang, W., Crystal-Plane-controlled Surface Restructuring and Catalytic Performance of Oxide Nanocrystals, Angewandte Chemie International Edition, Vol. 50, No. 51, p. 12294-12298, 2017.

Belin, T. and Epron, F., Characterization Methods of Carbon Nanotubes: a Review, Materials Science and Engineering: B, Vol. 119, No. 2, p. 105-118, 2005.

Bratan, V., Munteanu, C., Hornoiu, C., Vasile, A., Papa, F., State, R., Preda, S., Culita D., and Ionescu, N. I., CO Oxidation over Pd Supported Catalysts: In Situ Study of the Electric and Catalytic Properties, Applied Catalysis B: Environmental, Vol. 207 (Supplement C), p. 166-173, 2017.

Chai, S., Bai, X., Li, J., Liu, C., Ding, T., Tian, Y., Liu, C., Xian, H., Mi W., and Li, X., Effect of Phase Interaction on Catalytic CO Oxidation over the SnO_2/Al_2O_3 Model Catalyst, Applied Surface Science, Vol.402 (Supplement C), p. 12-20, 2017.

Chaunchaiyakul, S., Yano, T., Khoklang, K., Krukowski, P., Akai-Kasaya, M., Saito A., and Kuwahara, Y., Nanoscale Analysis of Multi-walled Carbon Nanotube by Tip-enhanced Raman Spectroscopy, Carbon, Vol. 99 (Supplement C), p. 642-648, 2016.

Chen, H., Yang, M., Tao S., and Chen, G., Oxygen Vacancy Enhanced Catalytic Activity of Reduced Co_3O_4 towards p-Nitrophenol Reduction, Applied Catalysis B: Environmental, Vol. 209 (Supplement C), p. 648-656, 2017.

Chen, Z., Wang, S., Liu, W., Gao, X., Gao, D., Wang M., and Wang, S., Morphology-dependent Performance of Co_3O_4 via Facile and Controllable Synthesis for Methane Combustion, Applied Catalysis A: General, Vol. 525 (Supplement C), p. 94-102, 2016.

Chuang, K. H., Lu, C. Y., Wey M. Y., and Huang, Y.-N., NO Removal by Activated Carbon-supported Copper Catalysts Prepared by Impregnation, Polyol, and Microwave Heated Polyol Processes, Applied Catalysis A: General, Vol. 397, No. 1 p. 234-240, 2011.

Cui, L., Zhao, D., Yang, Y., Wang Y., and Zhang, X., Synthesis of Highly Efficient α-Fe_2O_3 Catalysts for CO Oxidation Derived from MIL-100(Fe), Journal of Solid State Chemistry, Vol. 247 (Supplement C), p. 168-172, 2017.

Dong, F., Zhao, Y., Han, W., Zhao, H., Lu, G., and Tang, Z., Co Nanoparticles Anchoring Three Dimensional Graphene Lattice as Bifunctional Catalyst for Low-temperature CO Oxidation, Molecular Catalysis, Vol. 439 (Supplement C), p. 118-127, 2017.

Fattahi, M., Kazemeini, M., Khorasheh, F., and Rashidi, A. M., Morphological Investigations of Nanostructured V_2O_5 over Graphene Used for the ODHP Reaction: from Synthesis to Physiochemical Evaluations, Catalysis Science and Technology, Vol. 5, p. 910-924, 2015.

Gao, Y., Xie, K., Wang, W., Mi, S., Liu, N., Pan, G., and Huang, W., Structural Features and Catalytic Performance in CO Preferential Oxidation of CuO-CeO_2 Supported on Multi-walled Carbon Nanotubes, Catalysis Science and Technology, Vol. 5, No. 3, p. 1568-1579, 2015.

Huang, B., Huang, R., Jin, D., and Ye, D., Low Temperature SCR of NO with NH_3 over Carbon Nanotubes Supported Vanadium Oxides, Catalysis Today, Vol. 126, No. 3, p. 279-283, 2007.

Jin, M., Park, J. N., Shon, J. K., Kim, J. H., Li, Z., Park, Y. K., and Kim, J. M., Low Temperature CO Oxidation over Pd Catalysts Supported on Highly Ordered Mesoporous Metal Oxides, Catalysis Today, Vol. 185, No. 1, p. 183-190, 2012.

Kant Sh., Gautam, R., P., Kumar A., and Mandal K. D., Synthesis of Sphere-like Nano-crystalline Co_3O_4 Spinel via a Simple Homogeneous Precipitation Method, Materials Today: Proceedings, Vol. 4, No. 4, Part E, p. 5667-5671, 2017.

Kundu, S., Wang, Y., Xia, W., and Muhler, M., Thermal Stability and Reducibility of Oxygen-Containing Functional Groups on Multi-walled Carbon Nanotube Surfaces: A Quantitative High-resolution XPS and TPD/TPR Study, The Journal of Physical Chemistry C, Vol. 112, No. 43, p. 16869-16878, 2008.

Lee, S., Kang, J. S., Leung, K. T., Kim, S. K., and Sohn, Y., Magnetic Ni-Co Alloys Induced by Water Gas Shift Reaction, Ni-Co Oxides by CO Oxidation and their Supercapacitor Applications, Applied Surface Science, Vol. 386 (Supplement C), p. 393-404, 2016.

Liu, C., Gong, L., Dai, R., Lu, M., Sun, T., Liu, Q., Huang, X., and Huang, Z., Mesoporous Mn Promoted Co_3O_4 Oxides as an Efficient and Stable Catalyst for Low Temperature Oxidation of CO, Solid State Sciences, Vol. 71 (Supplement C) p. 69-74, 2017.

Liu, R., Liu, R., Ma, X., Davis, B. H., and Li, Z., Efficient Diesel Production over the Iron-based Fischer–Tropsch Catalyst Supported on CNTs Treated by Urea/NaOH Fuel, Vol. 211**,** p.827-836, 2018.

Lv, S., Xia, G., Jin, C., Hao, C., Wang, L., Li, J., Zhang Y., and Zhu, J. J., Low-temperature CO Oxidation by Co_3O_4 Nanocubes on the Surface of $Co(OH)_2$ Nanosheets, Catalysis Communications, Vol. 86 (Supplement C), p. 100-103, 2016.

Mazov, I., Kuznetsov, V. L., Simonova, I. A., Stadnichenko, A. I., Ishchenko, A. V., Romanenko, A. I., Tkachev, E. N., and Anikeeva, O. B., Oxidation Behavior of Multiwall Carbon Nanotubes with Different Diameters and Morphology, Applied Surface Science, Vol. 258, No. 17, p. 6272-6280, 2012.

Payan, A., Fattahi, M., Jorfi, S., Roozbehani, B., and Payan, S., Synthesis and Characterization of Titanate nanotube/Single-walled Carbon Nanotube (TNT/SWCNT) Porous Nanocomposite and its Photocatalytic Activity on 4-Chlorophenol Degradation under UV and Solar Irradiation. Applied Surface Science, Vol. 434, p. 336-350, 2018.

Pu, Z., Zhou, H., Zheng, Y., Huang, W., and Li, X., Enhanced Methane Combustion over Co_3O_4 Catalysts Prepared by a Facile Precipitation Method: Effect of Aging Time, Applied Surface Science, Vol. 410 (Supplement C), p. 14-21, 2017.

Qiao, B., Liang, J. X., Wang, A., Liu, J., and Zhang, T., Single Atom Gold Catalysts for Low-temperature CO Oxidation, Chinese Journal of Catalysis, Vol. 37, No. 10, p. 1580-1586, 2016.

Rashidi, A. M., Akbarnejad, M. M., Khodadadi, A. A., Mortazavi, Y., and Ali, A., Single-wall Carbon Nanotubes Synthesized Using Organic Additives to Co–Mo Catalysts Supported on Nanoporous MgO, Nanotechnology, Vol. 18, No. 31, p. 315605, 2007.

Santillan-Jimenez, E., Miljkovic-Kocic, V., Crocker, M., and Wilson, K., Carbon Nanotube-supported Metal Catalysts for NOx Reduction using Hydrocarbon Reductants. Part 1: Catalyst Preparation, Characterization and NOx reduction Characteristics, Applied Catalysis B: Environmental, Vol. 102, No. 1, p. 1-8, 2011.

Tang, C. W., Wang, C. B., and Chien, S. H., Characterization of Cobalt Oxides Studied by FT-IR, Raman, TPR and TG-MS, Thermochimica Acta, Vol. 473, No. 1, p. 68-73, 2008.

Wang, F., Effect of Support Carbon Materials on Ag Catalysts Used for CO Oxidation in the Presence and absence of H_2, Journal of Environmental Chemical Engineering, Vol. 4, No. 4, Part A, p. 4258-4262, 2016.

Wang, F., Zhang, L., Xu, L., Deng, Z., and Shi, W., Low Temperature CO Oxidation and CH_4 Combustion over Co_3O_4 Nanosheets, Fuel, Vol. 203 (Supplement C), p. 419-429, 2017.

Xia, Y., Dai, H., Jiang, H., and Zhang, L., Three-dimensional Ordered Mesoporous Cobalt Oxides: Highly Active Catalysts for the Oxidation of Toluene and Methanol, Catalysis Communications, Vol. 11, No. 15, p. 1171-1175, 2010.

Xing, Y., Li, L., Chusuei, C. C., and Hull, R. V., Sonochemical Oxidation of Multi-walled Carbon Nanotubes, Langmuir, Vol. 21, No. 9, p. 4185-4190, 2005.

Xiong, H., Motchelaho, M. A. M., Moyo, M., Jewell, L. L., and Coville, N. J., Cobalt Catalysts Supported on a Micro-coil Carbon in Fischer–Tropsch Synthesis: A Comparison with CNTs and CNFs, Catalysis Today, Vol. 214 (Supplement C), p. 50-60, 2013.

Yuan, C., Wang, H. G., Liu, J., Wu, Q., Duan, Q., and Li, Y., Facile Synthesis of Co_3O_4-CeO_2 Composite Oxide Nanotubes and their Multifunctional Applications for Lithium Ion Batteries and CO Oxidation, Journal of Colloid and Interface Science, Vol. 494 (Supplement C), p. 274-281, 2017.

Zhang, Y. C., Pan, L., Lu, J., Song, J., Li, Z., Zhang, X., Wang, L., and Zou, J. J., Unraveling the Facet-dependent and Oxygen Vacancy Role for Ethylene Hydrogenation on Co_3O_4 (110) Surface: A DFT$^+$U study, Applied Surface Science, Vol. 401 (Supplement C), p. 241-247, 2017.

Zhou, M., Li, J., Wang, K., Xia, H., Xu, J., and Jiang, J., Selective Conversion of Furfural to Cyclopentanone over CNT-supported Cu Based Catalysts: Model Reaction for Upgrading of Bio-oil, Fuel, Vol. 202, p. 1-11, 2017.

Zou, W., Du, Z. J., Liu, Y. X., Yang, X., Li, H. Q., and Zhang, C., Functionalization of MWNTs Using Polyacryloyl Chloride and the Properties of CNT–epoxy Matrix Nanocomposites, Composites Science and Technology, Vol. 68, No. 15, p. 3259-3264, 2008.